

Article

Flotation Separation of Chalcopyrite and Molybdenite Assisted by Microencapsulation Using Ferrous and Phosphate Ions: Part II. Flotation

Ilhwan Park ^{1,*}, Seungwan Hong ², Sanghee Jeon ¹, Mayumi Ito ¹ and Naoki Hiroyoshi ¹

¹ Division of Sustainable Resources Engineering, Faculty of Engineering, Hokkaido University, Sapporo 060-8628, Japan; shjun1121@eng.hokudai.ac.jp (S.J.); itomayu@eng.hokudai.ac.jp (M.I.); hiroyosi@eng.hokudai.ac.jp (N.H.)

² Cooperative Program for Resources Engineering, Graduate School of Engineering, Hokkaido University, Sapporo 060-8628, Japan; seungwan.hong.s4@elms.hokudai.ac.jp

* Correspondence: i-park@eng.hokudai.ac.jp; Tel.: +81-11-706-6315

Abstract: Porphyry-type deposits are the major sources of copper and molybdenum, and flotation has been adopted to recover them separately. The conventional reagents used for depressing copper minerals, such as NaHS, Na₂S, and Nokes reagent, have the potential to emit toxic H₂S gas when pulp pH was not properly controlled. Thus, in this study the applicability of microencapsulation (ME) using ferrous and phosphate ions as an alternative process to depress the floatability of chalcopyrite was investigated. During ME treatment, the use of high concentrations of ferrous and phosphate ions together with air introduction increased the amount of FePO₄ coating formed on the chalcopyrite surface, which was proportional to the degree of depression of its floatability. Although ME treatment also reduced the floatability of molybdenite, ~92% Mo could be recovered by utilizing emulsified kerosene. Flotation of chalcopyrite/molybdenite mixture confirmed that the separation efficiency was greatly improved from 10.9% to 66.8% by employing ME treatment as a conditioning process for Cu-Mo flotation separation.

Keywords: porphyry deposits; chalcopyrite; molybdenite; microencapsulation; flotation



Citation: Park, I.; Hong, S.; Jeon, S.; Ito, M.; Hiroyoshi, N. Flotation Separation of Chalcopyrite and Molybdenite Assisted by Microencapsulation Using Ferrous and Phosphate Ions: Part II. Flotation. *Metals* **2021**, *11*, 439. <https://doi.org/10.3390/met11030439>

Academic Editor: Man Seung Lee

Received: 19 February 2021

Accepted: 5 March 2021

Published: 7 March 2021

Publisher's Note: MDPI stays neutral with regard to jurisdictional claims in published maps and institutional affiliations.



Copyright: © 2021 by the authors. Licensee MDPI, Basel, Switzerland. This article is an open access article distributed under the terms and conditions of the Creative Commons Attribution (CC BY) license (<https://creativecommons.org/licenses/by/4.0/>).

1. Introduction

Porphyry-type deposits are the major sources of copper (Cu) and molybdenum (Mo)—approximately 60% of Cu and 50% of Mo are annually produced from these deposits [1–3]. Apart from Cu and Mo, precious metals (e.g., gold (Au), silver (Ag), and platinum group elements (PGEs)) and several strategic/high-tech elements (e.g., rhenium (Re), tungsten (W), bismuth (Bi), indium (In), tellurium (Te), and selenium (Se)) may reach economic concentrations, thus being recovered as by-products during porphyry ore processing [3,4]. Typically, porphyry-type deposits are developed via a series of processes: (i) open-pit mining to excavate the ores, (ii) closed-circuit comminution to liberate valuable and non-valuable minerals, (iii) bulk flotation to recover Cu and Mo minerals (i.e., mainly chalcopyrite (CuFeS₂) and molybdenite (MoS₂)) as Cu-Mo bulk concentrates, and (iv) Mo flotation to separate Cu and Mo minerals from bulk concentrates [2].

At the final stage of porphyry ore processing (i.e., flotation separation of Cu and Mo minerals), Cu-Mo bulk concentrates are conditioned with Cu depressants (e.g., sodium hydrosulfide (NaHS), sodium sulfide (Na₂S), and Nokes reagent (P₂S₅ + NaOH)) to reduce the floatability of chalcopyrite while floating molybdenite [1,2]. Although effective, these reagents have the potential to emit hydrogen sulfide (H₂S) gas—known as toxic and deadly gas—when the pulp pH is not properly maintained; for example, at pH < 10, HS[−] ion derived from Cu depressants starts forming H₂S_(aq) species, which is then readily transformed into the gaseous phase, i.e., H₂S_(g), due to its extremely high vapor pressure (P_{H₂S} = 20.03 atm at 25 °C) [2,5]. To avoid the accident that is caused by H₂S emission, the

flotation circuits should consist of covered flotation cells together with active ventilation systems as well as a NaOH-solution scrubber treating any process off-gas [6]. However, the use of covered flotation cells obviously obstructs visual inspection of the froth, which lowers the efficiency of operations of flotation process [6]. Not only this, but the use of above-mentioned reagents may destroy the pipelines due to the corrosive nature of H₂S and yield imperfect molybdenite recovery [7–9], so the attention should be paid to the development of alternative techniques.

This paper is Part II of a two-part basic study to investigate how the application of microencapsulation technique affects flotation behaviors of chalcopyrite and molybdenite. Microencapsulation is a technique that encloses the target material with coatings composed of small discrete solid particles or small liquid droplets. It has been reported that microencapsulation using redox-sensitive compounds has an ability to selectively form the coating on the surface of conductive minerals [10–14]. In Part I of this study, microencapsulation using ferrous and phosphate ions was investigated with the aim of creating ferric phosphate (FePO₄) coating selectively on the chalcopyrite surface [15]. Electrochemical study revealed that ferrous oxidation occurred preferably on the surface of chalcopyrite rather than molybdenite. Moreover, the results of shake-flask experiments coupled with surface characterizations were consistent with electrochemical study; that is, ferrous oxidation followed by FePO₄ formation occurred predominantly on the chalcopyrite surface. However, it remains unclear how FePO₄ coating formed via microencapsulation affects the floatability of chalcopyrite and molybdenite. In Part II, thus, flotation tests of chalcopyrite and/or molybdenite with and without microencapsulation treatment were carried out to evaluate its effect on the floatability of chalcopyrite and molybdenite as well as their separation efficiency.

2. Materials and Methods

2.1. Mineral Samples

Chalcopyrite and molybdenite were obtained from Copper Queen Mine, Cochise County, AZ, USA and Spain Mine, Renfrew County, ON, Canada, respectively. The samples were crushed by a jaw crusher (BB 51, Retsch Inc. Haan, Germany), ground by a vibratory disc mill (RS 100, Retsch Inc., Haan, Germany), and then screened in order to obtain a size fraction of 38–75 µm. Chalcopyrite sample mainly consists of chalcopyrite (~70%) with minor amounts of impurities like pyrite (FeS₂) and silicate minerals (e.g., quartz (SiO₂), amesite (Mg₂Al₂SiO₅(OH)₄), and actinolite (Ca₂(Mg, Fe²⁺)₅Si₈O₂₂(OH)₂)), while molybdenite sample is highly pure (~99.8%). The detailed sample characterizations can be found in Part I of this study [15].

2.2. Microencapsulation Treatment

Prior to microencapsulation (ME) treatment, mineral samples were deslimed by ultrasonication in ethanol for 1 min, followed by decantation after 1 min sedimentation. Afterward, the sediments were rinsed with acetone four times and dried in vacuum desiccators.

Microencapsulation treatments were conducted using an agitator-type flotation machine (FT-1000, Heiko, Japan). In a 400-mL flotation cell, 20 g of mineral sample (i.e., chalcopyrite, molybdenite, or chalcopyrite/molybdenite mixture (1:1, *w/w*)) and 200 mL of coating solution containing ferrous and phosphate ions were mixed at 1000 rpm for 1 h. Coating solution was prepared using FeSO₄·7H₂O and KH₂PO₄, and its pH was adjusted to 4.0 ± 0.1 while using dilute HCl and NaOH. All the chemicals used in this study were of reagent grade (Wako Pure Chemical Industries, Ltd., Osaka, Japan). To investigate the suitable conditions for depressing the floatability of chalcopyrite, the effects of the concentrations of ferrous and phosphate ions (1 and 10 mM) and the introduction of air (1 L/min) during ME treatment were examined.

After ME treatment, the suspension was filtered and washed with deionized (DI) water 4 times to remove the remaining ferrous and phosphate ions, and then used for flotation experiments. Filtrates were collected using 0.2 µm syringe-driven filters (LMS Co. Ltd.,

Tokyo, Japan) and analyzed by inductively coupled plasma atomic emission spectrometer (ICP-AES, ICPE9820, Shimadzu Corporation, Kyoto, Japan) in order to identify the changes in dissolved Fe and P concentrations.

2.3. Flotation Tests

Flotation tests were conducted using an agitator-type flotation machine (FT-1000, Heiko, Japan) equipped with a 400-mL flotation cell in which 20 g of washed sample, 10 g of quartz (99.9% SiO₂, Wako Pure Chemical Industries, Ltd., Osaka, Japan), and 400 mL DI water were added. The purpose of adding quartz is to measure the amounts of chalcopyrite/molybdenite recovered by entrainment. The pulp was suspended at 1000 rpm for 3 min, and then conditioned with 25 µL/L of frother (methyl isobutyl carbinol, MIBC, Tokyo Chemical Industry Co., Ltd., Tokyo, Japan) for another 3 min. In the flotation of molybdenite and chalcopyrite/molybdenite mixture, 2.5 L/t of emulsified kerosene was added as a collector for molybdenite and conditioned for 3 min. Emulsified kerosene was prepared as follows: (i) kerosene (Wako Pure Chemical Industries, Ltd., Osaka, Japan) was mixed with distilled water in the concentration of 20 wt.%; (ii) emulsification was carried out using an ultrasonic homogenizer (ULTRA-TURRAX, IKA, Königswinter, Germany) for 60 s [16,17]. Afterward, air was injected into the suspension at a flow rate of 1 L/min, and flotation was carried out for 3 min (for the case of flotation of chalcopyrite/molybdenite mixture, it was conducted for up to 6 min). Froth products and tailings obtained after flotation were weighed after drying at 105 °C for 24 h, and their elemental compositions were determined using X-ray fluorescence spectrometer (XRF, EDXL300, Rigaku Corporation, Tokyo, Japan).

2.4. Contact Angle Measurements

Contact angle measurements were carried out in order to estimate the changes in the surface wettability of molybdenite before and after ME treatment (with and without kerosene addition). For this, molybdenite specimen was cut using a diamond cutter to obtain a small cuboid crystal (~5 mm (w) × 5 mm (d) × 10 mm (h)), which was then polished using a polishing machine (SAPHIR 250 M1, ATM GmbH, Mammelzen, Germany) with a series of silicon carbide papers (P320, P600, and P1200) and diamond suspensions (3 and 1 µm). Afterward, the contact angles of (i) untreated molybdenite, (ii) ME-treated molybdenite with 10 mM Fe²⁺/H₂PO₄⁻ at 1 L/min air introduction for 1 h, and (iii) ME-treated molybdenite with conditioning using 2.5 L/t of emulsified kerosene for 3 min were measured by a high-magnification digital microscope (VHX-1000, Keyence Corporation, Osaka, Japan) with built in image analysis capability. Each measurement was repeated 3 times at different spots on the mineral surface to ascertain that the differences observed were statistically significant.

3. Results and Discussion

3.1. Flotation of Chalcopyrite

Figure 1 shows the effect of ME treatment on the floatability of chalcopyrite. For the case of untreated chalcopyrite, about 77% of Cu was recovered after 3 min flotation even in the absence of any collector. When chalcopyrite was treated by ME with 1 mM Fe²⁺ and 1 mM H₂PO₄⁻ prior to flotation, Cu recovery was almost the same as the one without ME treatment. In Part I of this study [15], it was confirmed that after ME treatment using 1 mM Fe²⁺ and 1 mM H₂PO₄⁻, chalcopyrite was obviously coated with FePO₄; however, its floatability was not affected by FePO₄ coating.

One of the possible reasons for why ME treatment did not affect the floatability of chalcopyrite could be due to the insufficient amount of FePO₄ coating for depressing chalcopyrite. After 1 h ME treatment, ~80% of dissolved Fe and P were precipitated as FePO₄, indicating that the wt.% of FePO₄ present on the chalcopyrite surface was approximately 0.12% [15]. If chalcopyrite is covered with a large amount of FePO₄ coating (i.e., >0.12%), its floatability may be decreased. Thus, an attempt was made to increase the amount of

FePO₄ coating formed on the chalcopyrite surface by increasing the concentrations of Fe²⁺ and H₂PO₄⁻ from 1 to 10 mM during ME treatment. As shown in Figure 2, Cu recovery was decreased from ~80% to ~70% when Fe²⁺/H₂PO₄⁻ concentrations increased from 1 to 10 mM. Although increasing Fe²⁺/H₂PO₄⁻ concentrations during ME treatment could reduce the floatability of chalcopyrite, the degree of chalcopyrite depression is not enough for separating chalcopyrite and molybdenite.

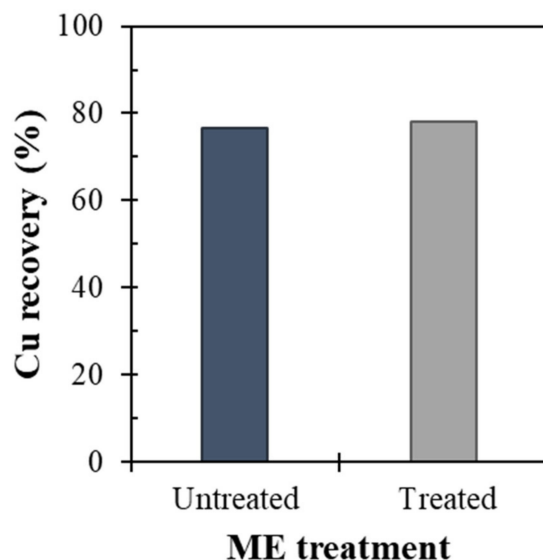


Figure 1. Effect of ME treatment on the floatability of chalcopyrite.

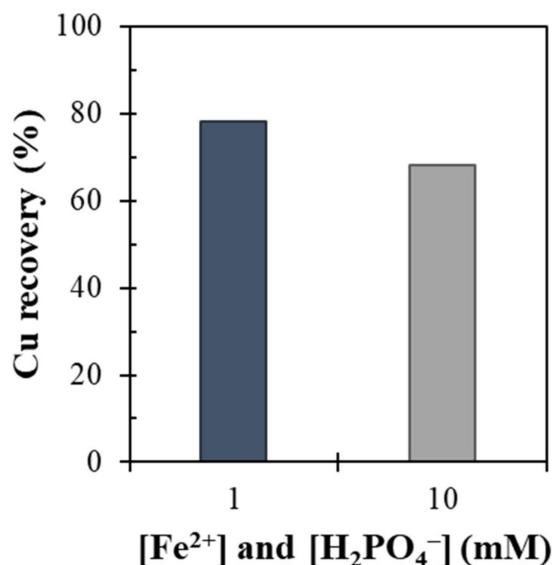
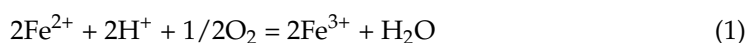


Figure 2. Effect of the concentration of Fe²⁺ and H₂PO₄⁻ on the floatability of chalcopyrite.

The concentration of FePO₄ formed after ME treatment was 0.66 mM for the case using 1 mM Fe²⁺/H₂PO₄⁻, while ~1 mM of FePO₄ was formed when 10 mM Fe²⁺/H₂PO₄⁻ was used. These results support our deduction that increasing the amount of FePO₄ coating can enhance the depression of chalcopyrite. However, there are large amounts of unreacted ferrous and phosphate ions that remained in the solution after ME treatment. As illustrated in Equation (1), oxygen is an essential reactant for ferrous oxidation.



To facilitate the formation of more coatings on the surface of chalcopyrite, thus, the air was introduced during ME treatment in the presence of 10 mM $\text{Fe}^{2+}/\text{H}_2\text{PO}_4^-$. As shown in Figure 3, air introduction during ME treatment obviously improved the depression of chalcopyrite floatability; that is, Cu recovery decreased from about 70% (without air introduction) to <15% (with air introduction). Control experiment—flotation of chalcopyrite treated under air introduction (1 L/min) for 1 h in the absence of $\text{Fe}^{2+}/\text{H}_2\text{PO}_4^-$ —confirmed that air introduction did not play an important role in depressing the floatability of chalcopyrite because Cu recovery was almost the same as that of untreated chalcopyrite (data not shown). The main role of introducing air is to promote the cathodic half-cell reaction occurring on the surface of chalcopyrite (i.e., oxygen reduction reaction; Equation (2)), thereby enhancing the anodic half-cell reaction (i.e., ferrous oxidation reaction; Equation (3)). When the air was injected during ME treatment, ~4 mM of FePO_4 was formed, indicating that the formation of large amounts of FePO_4 coating is effective in depressing chalcopyrite.

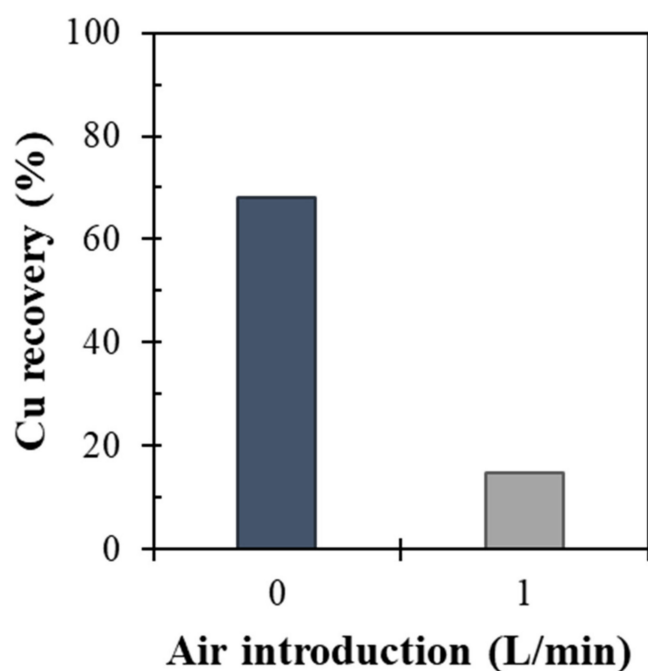
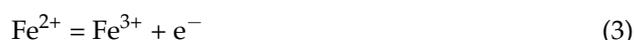


Figure 3. Effect of air introduction during ME treatment with 10 mM $\text{Fe}^{2+}/\text{H}_2\text{PO}_4^-$ on the floatability of chalcopyrite.

3.2. Flotation of Molybdenite

The main purpose of ME treatment is to depress the floatability of chalcopyrite, so molybdenite was also treated by ME under the same conditions where chalcopyrite was effectively depressed (i.e., 10 mM $\text{Fe}^{2+}/\text{H}_2\text{PO}_4^-$; 1 L/min air introduction). As shown in Figure 4, ME treatment had a detrimental effect on the floatability of molybdenite; that is, after ME treatment, Mo recovery decreased from ~45% to ~6%. For the flotation separation of chalcopyrite and molybdenite, the former should be depressed while floating the latter; thus, this is an unwelcome result because molybdenite was also depressed after ME treatment. As confirmed by XPS analysis of ME-treated chalcopyrite and molybdenite shown in Part I of this study [15], the amount of FePO_4 coating formed on the molybdenite surface was obviously smaller than that formed on the chalcopyrite surface; however, molybdenite was strongly depressed as much as chalcopyrite was (Figures 3 and 4).

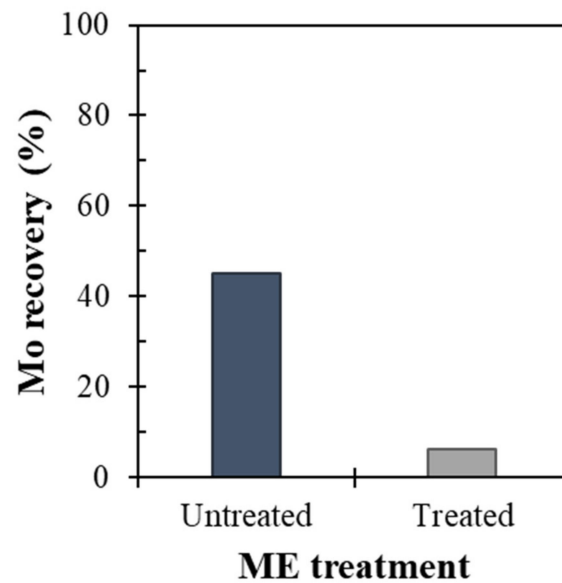


Figure 4. Effect of ME treatment on the floatability of molybdenite. Note that ME treatment was conducted with 10 mM $\text{Fe}^{2+}/\text{H}_2\text{PO}_4^-$ and 1 L/min air introduction.

The presence of precipitates on the molybdenite surface has been reported to reduce its floatability; for example, (i) flotation of Cu-Mo ores in seawater where seawater precipitates (e.g., $\text{Mg}(\text{OH})_2$ and CaCO_3) formed at $\text{pH} > 9.5$ are accumulated on the molybdenite surface [18–21]; (ii) flotation of chalcopyrite/molybdenite mixture after plasma pretreatment resulting in the formation of Cu/Fe oxyhydroxides on the surface of molybdenite [22]. Hirajima and coworkers [20–22] reported that the reduced floatability of molybdenite caused by precipitates can be healed by adding kerosene—a commonly used collector for molybdenite. In this study, thus, kerosene was also adopted after ME treatment to improve the recovery of molybdenite. As can be seen in Figure 5, the addition of kerosene was remarkably effective in improving the floatability of ME-treated molybdenite; that is, Mo recovery was increased from ~6% to ~92% when 2.5 L/t of kerosene was added.

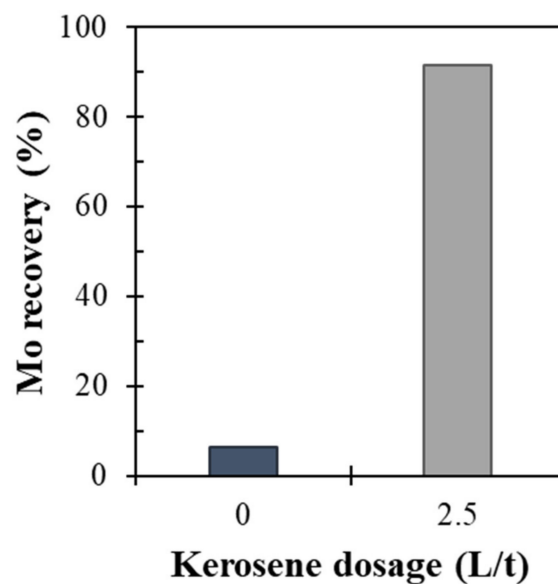


Figure 5. Effect of kerosene dosage on the floatability of ME-treated molybdenite.

The increased Mo recovery achieved by kerosene addition most likely resulted from the improvement of hydrophobicity of molybdenite surface. As illustrated in Figure 6,

the contact angle of untreated molybdenite was $\sim 94^\circ$ but decreased to $\sim 39^\circ$ after ME treatment due to the presence of hydrophilic FePO_4 precipitates on its surface. When ME-treated molybdenite reacted with kerosene, however, the contact angle increased to $\sim 109^\circ$, indicating that the hydrophobicity of molybdenite was improved, even better than that of bare molybdenite surface. This increased hydrophobicity of ME-treated molybdenite can be explained as follows: kerosene is adsorbed on molybdenite surface where FePO_4 is not present and/or covers not only molybdenite but also the attached FePO_4 precipitates.

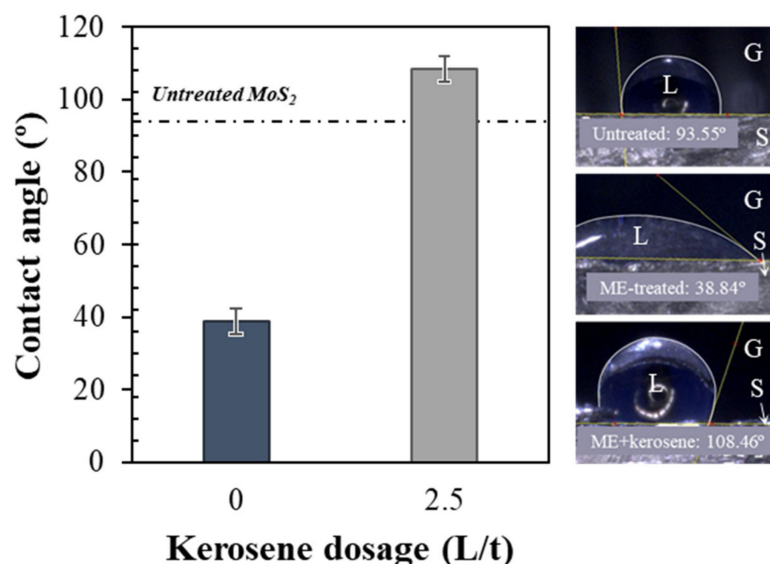


Figure 6. Effect of kerosene dosage on the contact angle of ME-treated molybdenite. Note that G, L, and S on the right side of the photos indicate gas (air), liquid (water droplet), and solid (molybdenite) phases, respectively.

Based on the results of Sections 3.1 and 3.2, Cu-Mo flotation separation could be achievable under the following conditions: ME treatment with 10 mM $\text{Fe}^{2+}/\text{H}_2\text{PO}_4^-$ while introducing air at 1 L/min air introduction, and flotation with 2.5 L/t kerosene. Although ME treatment followed by flotation of single minerals (i.e., chalcopyrite or molybdenite) looked promising, flotation results can be differed when they are mixed, so the following section deals with the mixed minerals system.

3.3. Flotation of Chalcopyrite/Molybdenite Mixture

Figure 7 shows flotation results of chalcopyrite/molybdenite mixture with and without ME treatment. As illustrated in Figure 7a, flotation of untreated chalcopyrite/molybdenite mixture showed that both minerals were floated well and, after 6 min flotation, the recovery of Cu and Mo reached about 83% and 92%, respectively. On the other hand, Cu and Mo recoveries after 6 min flotation of ME-treated mixture were $\sim 33\%$ and $\sim 93\%$, respectively (Figure 7b). In the case of ME-treated mixture, froth products with higher Mo grade (46.33–49.3%) and lower Cu grade (3.8–5.2%) compared to those of untreated mixture (i.e., Mo grade, 33.8–34.6%; Cu grade, 9.6–9.8%) were obtained. These results indicate that the application of ME treatment prior to flotation of chalcopyrite/molybdenite mixture could selectively depress the floatability of chalcopyrite.

The effect of ME treatment on flotation of chalcopyrite/molybdenite mixture was evaluated by the classical first-order flotation kinetic model (Equation (4)) [23]:

$$R(t) = R_\infty [1 - \exp(-kt)], \quad (4)$$

where $R(t)$ and R_∞ are the recovery of chalcopyrite/molybdenite at time t and an infinite time, and k is the first-order rate constant. A nonlinear least square regression was used to calculate R_∞ and k from the best fit with experimental data. The obtained R_∞ and k were

used for calculating the modified rate constant (Equation (5)) and the selectivity index of mineral I over mineral II (Equation (6)) [24]:

$$K_M = R_\infty \cdot k, \quad (5)$$

$$\text{S.I. (I/II)} = (K_M \text{ of mineral I}) / (K_M \text{ of mineral II}). \quad (6)$$

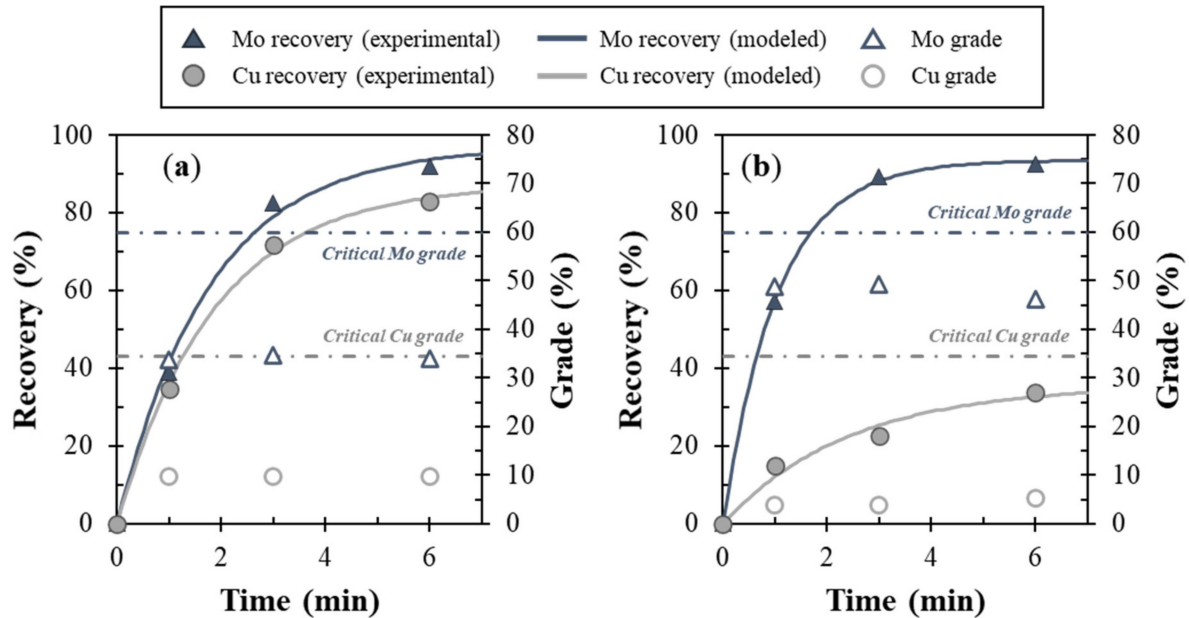


Figure 7. Effect of ME treatment on the floatability of chalcopyrite and molybdenite in the mixed mineral flotation: (a) untreated and (b) treated chalcopyrite/molybdenite mixture. Note that markers indicate experimental data while lines denote calculated values based on the first-order flotation kinetic model (Equation (4)).

The regression coefficients (e.g., R_∞ and k), K_M , and S.I. (Mo/Cu) were summarized in Table 1. The maximum recovery (R_∞) of molybdenite was almost the same irrespective of ME treatment (i.e., 97.0% without ME; 93.5% with ME), whereas R_∞ of ME-treated chalcopyrite decreased significantly from 87.3% to 35.7%. After ME treatment, the rate constant (k) and modified rate constant (K_M) increased for molybdenite but decreased for chalcopyrite. Moreover, the selectivity index of Mo/Cu of ME-treated chalcopyrite/molybdenite mixture was about five-fold higher than that of untreated mixture, indicating that ME treatment has an ability to selectively depress the floatability of chalcopyrite.

Table 1. Non-linear regression results for the first-order kinetic model fitting to the experimental data (Figure 6).

Parameters	Untreated		Treated	
	Chalcopyrite	Molybdenite	Chalcopyrite	Molybdenite
R^2	0.99	0.99	0.93	0.99
R_∞ (%)	87.3	97.0	35.7	93.5
k (min^{-1})	0.54	0.56	0.41	0.96
K_M (min^{-1})	0.47	0.54	0.15	0.89
S.I. (Mo/Cu)	1.16		6.08	

Figure 8 shows the relationship between Mo recovery in the froth and Cu recovery

in the tailing after flotation with and without ME treatment, which is often used for the assessment of the separation efficiency (Equation (7)) [16,25–27]:

$$\eta = R_c - (1 - R_t), \quad (7)$$

where η is Newton's efficiency, R_c is the recovery of molybdenite in the froth, and R_t is the recovery of chalcopyrite in the tailing. For the case of untreated chalcopyrite/molybdenite mixture, the separation efficiencies were in the range of 4.0–10.9% (Figure 8). Compared to this, the application of ME treatment greatly improved the separation efficiency. Until 3 min of flotation, Mo recovery was rapidly increased up to ~90% but, afterward, slightly increased up to 93.5%. On the other hand, Cu recovery was apparently lower than Mo recovery but continuously increased up to 35.7% with time, which results in the highest separation efficiency at 3 min. In short, the separation efficiencies of untreated and treated mixture obtained after 3 min flotation were 10.9% and 66.8%, respectively. This suggests that the application of ME treatment as a Cu depression process prior to Cu-Mo flotation separation is effective in improving Mo/Cu separation efficiency.

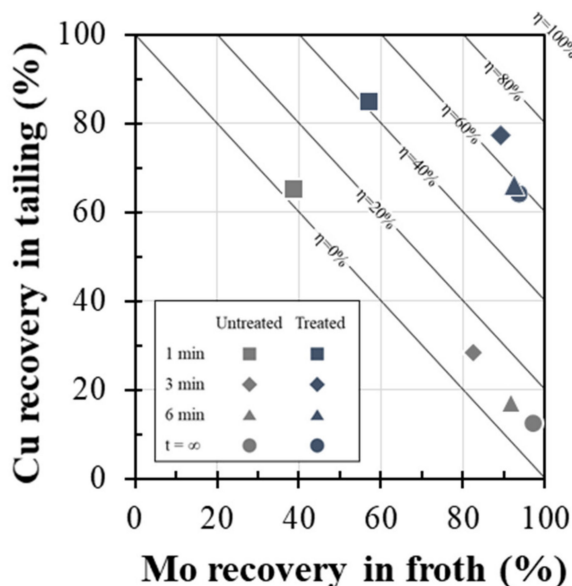


Figure 8. Relationship between Mo recovery in froth and Cu recovery in tailing obtained in the mixed mineral flotation.

4. Conclusions

This study investigated the effect of microencapsulation using $\text{Fe}^{2+}/\text{H}_2\text{PO}_4^-$ as a pretreatment for Cu-Mo flotation separation. The findings of this study are summarized, as follows:

1. ME treatment using 10 mM $\text{Fe}^{2+}/\text{H}_2\text{PO}_4^-$ had a negligible effect on the depression of chalcopyrite floatability, but air introduction during ME treatment dramatically reduced Cu recovery from ~70% to ~15%. The air introduction played an important role in enhancing ferrous oxidation occurring on the surface of chalcopyrite, thereby improving the formation of FePO_4 coating on its surface.
2. Not only chalcopyrite, but the floatability of molybdenite was also depressed after ME treatment. The reduced floatability of ME-treated molybdenite, however, could be improved by utilizing emulsified kerosene during flotation.
3. The application of ME treatment was also effective for mixed minerals system that the separation efficiency increased from 10.9% (without ME treatment) to 66.8% (with ME treatment).

Author Contributions: Conceptualization, I.P., S.J., M.I. and N.H.; methodology, I.P.; investigation, I.P. and S.H.; data curation, I.P. and S.H.; writing—original draft preparation, I.P.; writing—review and editing, I.P., S.H., S.J., M.I. and N.H.; funding acquisition, I.P. All authors have read and agreed to the published version of the manuscript.

Funding: This study is financially supported by Japan Oil, Gas and Metals National Corporation (JOGMEC).

Institutional Review Board Statement: Not applicable.

Informed Consent Statement: Not applicable.

Data Availability Statement: Data available on request due to restrictions, as the research is ongoing.

Conflicts of Interest: The authors declare no conflict of interest.

References

1. Bulatovic, S.M. 12-Flotation of Copper Sulfide Ores. In *Handbook of Flotation Reagents*; Bulatovic, S.M., Ed.; Elsevier: Amsterdam, The Netherlands, 2007; pp. 235–293. ISBN 978-0-444-53029-5.
2. Park, I.; Hong, S.; Jeon, S.; Ito, M.; Hiroyoshi, N. A Review of Recent Advances in Depression Techniques for Flotation Separation of Cu–Mo Sulfides in Porphyry Copper Deposits. *Metals* **2020**, *10*, 1269. [[CrossRef](#)]
3. John, D.A.; Ayuso, R.A.; Barton, M.D.; Blakely, R.J.; Bodnar, R.J.; Dilles, J.H.; Gray, F.; Graybeal, F.T.; Mars, J.L.; McPhee, D.K.; et al. *Porphyry Copper Deposit Model: Chapter B in Mineral Deposit Models for Resource Assessment*; Scientific Investigations Report 2010-5070-B; U.S. Geological Survey: Menlo Park, CA, USA, 2010; 169p.
4. Cioacă, M.-E.; Munteanu, M.; Lynch, E.P.; Arvanitidis, N.; Bergqvist, M.; Costin, G.; Ivanov, D.; Milu, V.; Arvidsson, R.; Iorga-Pavel, A.; et al. Mineralogical Setting of Precious Metals at the Assarel Porphyry Copper-Gold Deposit, Bulgaria, as Supporting Information for the Development of New Drill Core 3D XCT-XRF Scanning Technology. *Minerals* **2020**, *10*, 946. [[CrossRef](#)]
5. Stull, D.R. Vapor Pressure of Pure Substances. Organic and Inorganic Compounds. *Ind. Eng. Chem.* **1947**, *39*, 517–540. [[CrossRef](#)]
6. Amelunxen, P.; Schmitz, C.; Hill, H.; Goodweiler, N.; Andres, J. Molybdenum. In *SME Mineral Processing & Extractive Metallurgy Handbook*; Society for Mining, Metallurgy & Exploration (SME): Englewood, CO, USA, 2019; Volume 2, pp. 1891–1916.
7. Hirajima, T.; Miki, H.; Suyantara, G.P.W.; Matsuoka, H.; Elmahdy, A.M.; Sasaki, K.; Imaizumi, Y.; Kuroiwa, S. Selective Flotation of Chalcopyrite and Molybdenite with H₂O₂ Oxidation. *Miner. Eng.* **2017**, *100*, 83–92. [[CrossRef](#)]
8. Miki, H.; Matsuoka, H.; Hirajima, T.; Suyantara, G.P.W.; Sasaki, K. Electrolysis Oxidation of Chalcopyrite and Molybdenite for Selective Flotation. *Mater. Trans.* **2017**, *58*, 761–767. [[CrossRef](#)]
9. Yin, Z.; Sun, W.; Hu, Y.; Zhang, C.; Guan, Q.; Zhang, C. Separation of Molybdenite from Chalcopyrite in the Presence of Novel Depressant 4-Amino-3-Thioxo-3,4-Dihydro-1,2,4-Triazin-5(2H)-One. *Minerals* **2017**, *7*, 146. [[CrossRef](#)]
10. Park, I.; Tabelin, C.B.; Magaribuchi, K.; Seno, K.; Ito, M.; Hiroyoshi, N. Suppression of the Release of Arsenic from Arsenopyrite by Carrier-Microencapsulation Using Ti-Catechol Complex. *J. Hazard. Mater.* **2018**, *344*, 322–332. [[CrossRef](#)] [[PubMed](#)]
11. Park, I.; Tabelin, C.B.; Seno, K.; Jeon, S.; Ito, M.; Hiroyoshi, N. Simultaneous Suppression of Acid Mine Drainage Formation and Arsenic Release by Carrier-Microencapsulation Using Aluminum-Catecholate Complexes. *Chemosphere* **2018**, *205*, 414–425. [[CrossRef](#)] [[PubMed](#)]
12. Li, X.; Hiroyoshi, N.; Tabelin, C.B.; Naruwa, K.; Harada, C.; Ito, M. Suppressive Effects of Ferric-Catecholate Complexes on Pyrite Oxidation. *Chemosphere* **2019**, *214*, 70–78. [[CrossRef](#)] [[PubMed](#)]
13. Park, I.; Tabelin, C.B.; Seno, K.; Jeon, S.; Inano, H.; Ito, M.; Hiroyoshi, N. Carrier-Microencapsulation of Arsenopyrite Using Al-Catecholate Complex: Nature of Oxidation Products, Effects on Anodic and Cathodic Reactions, and Coating Stability under Simulated Weathering Conditions. *Heliyon* **2020**, *6*, e03189. [[CrossRef](#)] [[PubMed](#)]
14. Park, I.; Higuchi, K.; Tabelin, C.B.; Jeon, S.; Ito, M.; Hiroyoshi, N. Suppression of Arsenopyrite Oxidation by Microencapsulation Using Ferric-Catecholate Complexes and Phosphate. *Chemosphere* **2021**, *269*, 129413. [[CrossRef](#)] [[PubMed](#)]
15. Park, I.; Hong, S.; Jeon, S.; Ito, M.; Hiroyoshi, N. Flotation Separation of Chalcopyrite and Molybdenite Assisted by Microencapsulation Using Ferrous and Phosphate Ions: Part I. Selective Coating Formation. *Metals* **2020**, *10*, 1667. [[CrossRef](#)]
16. Hornn, V.; Ito, M.; Shimada, H.; Tabelin, C.B.; Jeon, S.; Park, I.; Hiroyoshi, N. Agglomeration-Flotation of Finely Ground Chalcopyrite and Quartz: Effects of Agitation Strength during Agglomeration Using Emulsified Oil on Chalcopyrite. *Minerals* **2020**, *10*, 380. [[CrossRef](#)]
17. Hornn, V.; Ito, M.; Shimada, H.; Tabelin, C.B.; Jeon, S.; Park, I.; Hiroyoshi, N. Agglomeration-Flotation of Finely Ground Chalcopyrite Using Emulsified Oil Stabilized by Emulsifiers: Implications for Porphyry Copper Ore Flotation. *Metals* **2020**, *10*, 912. [[CrossRef](#)]
18. Castro, S. Challenges in flotation of Cu–Co sulfide ores in sea water. In *The First International Symposium on Water in Mineral Processing*; Society for Mining, Metallurgy & Exploration (SME): Littleton, CO, USA, 2012; pp. 29–40.
19. Jeldres, R.I.; Arancibia-Bravo, M.P.; Reyes, A.; Aguirre, C.E.; Cortes, L.; Cisternas, L.A. The Impact of Seawater with Calcium and Magnesium Removal for the Flotation of Copper-Molybdenum Sulfide Ores. *Miner. Eng.* **2017**, *109*, 10–13. [[CrossRef](#)]

20. Hirajima, T.; Suyantara, G.P.W.; Ichikawa, O.; Elmahdy, A.M.; Miki, H.; Sasaki, K. Effect of Mg^{2+} and Ca^{2+} as Divalent Seawater Cations on the Floatability of Molybdenite and Chalcopyrite. *Miner. Eng.* **2016**, *96–97*, 83–93. [[CrossRef](#)]
21. Suyantara, G.P.W.; Hirajima, T.; Miki, H.; Sasaki, K. Floatability of Molybdenite and Chalcopyrite in Artificial Seawater. *Miner. Eng.* **2018**, *115*, 117–130. [[CrossRef](#)]
22. Hirajima, T.; Mori, M.; Ichikawa, O.; Sasaki, K.; Miki, H.; Farahat, M.; Sawada, M. Selective Flotation of Chalcopyrite and Molybdenite with Plasma Pre-Treatment. *Miner. Eng.* **2014**, *66–68*, 102–111. [[CrossRef](#)]
23. King, R.P. Flotation. In *Modeling and Simulation of Mineral Processing Systems*; Butterworth Heinemann: Oxford, UK, 2001; pp. 289–350.
24. Xu, M. Modified Flotation Rate Constant and Selectivity Index. *Miner. Eng.* **1998**, *11*, 271–278. [[CrossRef](#)]
25. Bilal, M.; Ito, M.; Koike, K.; Hornn, V.; Ul Hassan, F.; Jeon, S.; Park, I.; Hiroyoshi, N. Effects of Coarse Chalcopyrite on Flotation Behavior of Fine Chalcopyrite. *Miner. Eng.* **2021**, *163*, 106776. [[CrossRef](#)]
26. Farahat, M.; Hirajima, T.; Sasaki, K.; Doi, K. Adhesion of Escherichia Coli onto Quartz, Hematite and Corundum: Extended DLVO Theory and Flotation Behavior. *Colloids Surf. B Biointerfaces* **2009**, *74*, 140–149. [[CrossRef](#)] [[PubMed](#)]
27. Aikawa, K.; Ito, M.; Kusano, A.; Park, I.; Oki, T.; Takahashi, T.; Furuya, H.; Hiroyoshi, N. Flotation of Seafloor Massive Sulfide Ores: Combination of Surface Cleaning and Deactivation of Lead-Activated Sphalerite to Improve the Separation Efficiency of Chalcopyrite and Sphalerite. *Metals* **2021**, *11*, 253. [[CrossRef](#)]